Semiempirical Rate Equation for Solid State Polymerization of Poly(Ethylene Terephthalate)

BEN DUH

768 Jennifer Trail, Tallmadge, Ohio 44278

ABSTRACT: Solid-state polymerization (SSP) of poly(ethylene terephthalate) (PET) is characterized by two distinct features. First, there exists an ultimate or limiting intrinsic viscosity (*IV*). Second, the SSP rate varies with the prepolymer *IV*. Although there are several existing empirical rate equations and numerous published models for the SSP of PET, none can adequately describe these features. In this article, a simple semiempirical rate equation that aptly describes the behaviors of the SSP of PET is proposed. It is based on the assumptions that there are two categories of functional end groups, active and inactive end groups, and that the overall SSP follows a second order kinetics. Thus, the overall SSP rate is expressed as $-dC/dt = 2\,k_a\,(C - C_{ai})^2$, where C is the total end group concentration, t, the SSP time, k_a, the apparent reaction rate constant, and C_{ai}, the apparent inactive end group concentration. With this rate equation, the effects of all factors that influence the SSP rate are implicitly and conveniently accounted for by the two parameters, k_a and C_{ai}. For example, k_a increases, while C_{ai} decreases, with increasing SSP temperature, increasing prepolymer *IV*, and decreasing particle size. The proposed rate equation fits the *IV* or molecular weight build-up curves for the SSP of PET under various conditions very well, and can be extrapolated beyond data with reasonable accuracy. © 2002 John Wiley & Sons, Inc. J Appl Polym Sci 84: 857–870, 2002; DOI 10.1002/app.10370

Key words: kinetics; poly(ethylene terephthalate); solid-state polymerization; rate equations

INTRODUCTION

Solid-state polymerization (SSP) is an important step in the manufacture of high molecular weight poly(ethylene terephthalate) (PET) resins for bottle, food-tray, and tire-cord applications. First, a prepolymer with an intermediate molecular weight or intrinsic viscosity (*IV*) is produced from dimethyl terephthalate (DMT) and ethylene glycol (EG) or from terephthalic acid (TPA) and ethylene glycol by a melt-phase polymerization process. The prepolymer thus produced is then fur-

ther polymerized in the solid phase at a temperature substantially higher than the glass transition temperature but below the crystalline melting point in a stream of an inert gas (usually nitrogen) or under a vacuum. Within the SSP temperature range, the functional end groups of the polymer chains are sufficiently mobile and activated to collide and react with one another to further increase the molecular weight.

Characteristics of SSP of PET

The SSP of PET has a couple of peculiar characteristics because of the heterogeneous (partially crystalline) structure of the polymer under the SSP conditions as reported by Bamford and Wayne:[1]

Correspondence to: B. Duh (bduh@att.net).

1. For each prepolymer *IV* at each reaction temperature, there exists an ultimate or limiting *IV*. Once the ultimate *IV* is reached, the *IV* ceases to increase even if the SSP is continued. The ultimate *IV* increases with increasing prepolymer *IV* and SSP temperature.
2. The reaction rate constants and the SSP rate increase with increasing prepolymer *IV*.

Kinetics of SSP of PET

The SSP of PET comprises the following four steps: (1) diffusion of functional (OH and COOH) end groups, (2) collision and reaction of end groups, (3) diffusion of reaction byproducts from the interior to the surface of the polymer particle, and (4) diffusion of reaction byproducts from the particle surface into the bulk of the gas phase.

Steps 1 and 2 can be lumped together, for simplicity, as the reaction step. There are two types of polycondensation reactions in SSP, transesterification and esterification. Transesterification is the reaction between two hydroxyl ends with EG as the reaction byproduct, and esterification is the reaction between a carboxyl end and a hydroxyl end with water as the reaction byproduct.

What makes the SSP process unique is the first step. Unlike in a well-agitated gas or liquid system, two chain ends in solid PET must diffuse toward each other before they can collide and react with each other. Gaymans et al.[2] suggested that the distances between reactive end groups increase as the SSP proceeds, and eventually, the SSP becomes limited by end-group diffusion. Chen and Chen[3] developed a kinetic expression for end-group diffusion limited SSP to explain their experimental results. Devotta and Mashelkar[4] theorized that there exists a sphere of action within which the chain ends search for each other by a diffusion motion. Because the distance a chain end can travel under the SSP conditions is limited, the models proposed by the above authors can explain the diminishing apparent rate constant as reported by Bamford and Wayne.[1] However, none of these authors used rate equations that predicted the existence of the ultimate *IV* in their SSP models.

Deficiencies of Existing Kinetic Models for SSP of PET

There are numerous kinetic models for the SSP of PET with various degrees of sophistication and complexity. However, none are without limitations or deficiencies. The following are some of the reasons:

1. Ignoring esterification or all polycondensation reactions: Chen et al.[5] and Chang[6] used a pure diffusion model to describe the SSP of PET, totally ignoring the source terms, chemical reaction rates, in their mass transfer equations. They implied that the SSP was due to the diffusion of EG that exists in the prepolymer. However, according to Cai et al.,[7] the EG concentration in the initial amorphous PET prepolymer is 0.007–0.01%, and after drying at 160°C for 0.5 h, it drops to zero. This means that there would be hardly any significant increase in the molecular weight if SSP were due to the diffusion of EG because the prepolymer is usually dried before the SSP. The main thing these authors demonstrated is that the shapes of SSP curves can be quite similar to that of diffusion curves. Although practically all commercially produced PET prepolymers have substantial carboxyl concentrations with at least 15% of the total chain ends being carboxyl ends, many authors of PET SSP articles, including Bamford and Wayne,[1] Cai et al.,[7] and Ranvindranath and Mashelkar,[8] considered only transesterification in their SSP models.
2. Inadequate reaction rate equations: most authors who included chemical reaction(s) in their SSP models, including Bamford and Wayne,[1] Devotta and Mashelkar,[4] Cai et al.,[7] Ravindranath and Mashelkar,[8] Tang et al.,[9] Kang,[10] and Mallon and Ray,[11] used simple second-order rate equations for transesterification and esterification reactions. Thus, the forward reaction rate equations for transesterification, R_{tf}, and esterification, R_{ef}, are given as

$$R_{tf} = 2k_{tf}[\text{OH}]^2 \quad (1)$$

$$R_{ef} = 2k_{ef}[\text{OH}][\text{COOH}] \quad (2)$$

where k_{tf} and k_{ef} are forward reaction rate constants for transesterification and esterification, respectively. With these rate equations, the models cannot predict the existence of the ultimate *IV* or the leveling-

off of the *IV* build-up curve. For example, Mallon and Ray[11] conceded that one possible objection to their data fittings may be that the *IV* curves based on the data tend to flatten out at higher conversions while their model predicts continued polymerization. They attributed this to the inappropriate assumption that the diffusion constant is linear with respect to the amorphous fraction, ignoring the effect of the ever-changing morphology. However, I believe, the forms of the rate equations they used are the problem.

3. Unreliable values of parameters used in the models: the forward reaction rate constants used in the SSP models are usually extrapolated from melt polymerization data despite the pronouncedly different morphology of solid PET. Bamford and Wayne[1] reported that rate constants for SSP are greater than those extrapolated from melt polymerization kinetics. Many authors assumed that the equilibrium constants (used to calculate backward reaction rate constants from the forward reaction rate constants) are the same for melt polymerization and SSP even though SSP is usually conducted at temperatures at least 50°C below the melt polymerization temperatures. Furthermore, all of these authors ignored the fact that the reaction rate constants vary with prepolymer *IV*. The diffusivities of byproducts (EG and water) used in the SSP models are usually obtained by model calculation or parameter fitting of SSP data. Therefore, the diffusivity values used by different researchers can vary greatly. For example, the diffusivity of EG used or developed in different SSP articles can differ by up to three orders of magnitude (e.g., of the order of 10^{-9} to 10^{-6} cm^2/s at 230°C).

4. Unrealistic particle shapes: practically all current commercially produced PET resins are pelletized having a near cylindrical shape with a near elliptic cross-section. However, most authors used simple, regular particle shapes to simulate SSP. For example, Cai et al.[7] and Tang et al.[9] used a one-dimensional slab, Chang[6] and Ravindranath and Mashelkar[8] used a cube, and Chen et al.,[5] Kang,[10] and Mallon and Ray[11] used a sphere.

Obviously, all the existing SSP models have their merits. However, because of the reasons given above, the values they can predict most likely are of rough approximations, not withstanding all the complex equations employed. Although some of these models are supposed to be able to predict the *IV* at each point within the polymer particle, this is of little practical value because of unrealistic particle shapes used and because of the fact that only composite *IV* values are routinely measured in practice. Because it is extremely difficult and tedious to accurately measure the *IV* values at various points within a polymer particle, the point *IV* values determined with these models must be integrated to obtain the average particle *IV* values to compare with the experimental data. Furthermore, even if the calculated average particle *IV* values match the data well, there is still no guarantee that the calculated point *IV* values are accurate.

Having worked in the SSP field for almost 30 years, I realize that what SSP researchers need most in their day-to-day works is a simple, reliable empirical rate equation that can satisfactorily describe the SSP behaviors and predict the *IV* value at any time of the SSP. The purpose of this article is to provide such an empirical rate equation and to demonstrate how it can be satisfactorily applied to SSP under various conditions. Because the proposed empirical equation possesses some theoretical bases, it can be considered as a semiempirical equation.

Development of a Semiempirical SSP Rate Equation

Recently, Duh[12] developed a modified second-order kinetic model for the fluid-bed SSP of finely divided PET prepolymers with negligible carboxyl contents. Under the experimental condition, the SSP is reaction controlled and there is only one polycondensation reaction, transesterification. The proposed rate equation is given as

$$-\frac{dC}{dt} = 2k(C - C_i)^2 \qquad (3)$$

where C is the total end group concentration, t, the reaction time, k, the forward reaction rate constant, and C_i, the inactive end group concentration. The inactive end groups include chemically dead end groups and functional end groups that are firmly trapped in the crystalline struc-

ture and cannot participate in the reaction. The presence of the inactive end groups is the reason why there exists an ultimate *IV*—the inactive end group concentration determines the ultimate *IV*. This equation fits the SSP data very well and is capable of appropriately explaining the peculiar behaviors of SSP.

Surprisingly, a rate equation of the form of eq. (3) can also fit the experimental data of SSP in most cases, including that jointly controlled by reaction and diffusion, the most commonly practiced SSP of PET. Thus, an empirical SSP rate equation is obtained. Simply replacing the rate constant k with the apparent rate constant k_a and the inactive end group concentration C_i with the apparent inactive end group concentration C_{ai} leads to

$$-\frac{dC}{dt} = 2k_a (C - C_{ai})^2 \qquad (4)$$

This equation expresses the net solid-state polycondensation rate without making distinctions between hydroxyl ends and carboxyl ends. The effects of all factors, such as temperature, prepolymer *IV* and carboxyl concentration, particle size, diffusion resistance, morphology, backward reactions, and degradation reactions, etc., are lumped into the two parameters, k_a and C_{ai}. Note that C and C_{ai} in eq. (4) are composite quantities based on whole particle, not point quantities, and k_a represents the net reaction rate constant.

Integrating eq. (4) and using the initial condition, $C = C_0$ at $t = 0$, yields

$$\frac{1}{C - C_{ai}} - \frac{1}{C_0 - C_{ai}} = 2k_a t \qquad (5)$$

Solving for C yields

$$C = \frac{C_0 + 2k_a (C_0 - C_{ai})C_{ai}t}{1 + 2k_a (C_0 - C_{ai})t} \qquad (6)$$

According to this equation, as t approaches infinity, C approaches C_{ai}, which determines the ultimate *IV*.

Equation (5) can be rearranged to give

$$\frac{C_0 - C}{t} = 2k_a (C_0 - C_{ai})C$$

$$- 2k_a (C_0 - C_{ai})C_{ai} \qquad (7)$$

If the semiempirical rate equation fits the SSP data, the $(C_0 - C)/t$ vs. C plot is a straight line with

$$\text{Slope} = 2k_a(C_0 - C_a) \qquad (8)$$

Equation (7) also indicates that, at $t = \infty$, $(C_0 - C)/t = 0$, and $C = C_{ai}$, or

$$C \text{ intercept} = C_{ai} \qquad (9)$$

In the PET industry, the total end group concentration C is usually given in the unit of mol/10^6 g, mmol/kg, or μmol/g. For simplicity, μmol/g will be used in this article, although it is not the most widely used unit. Thus, C can be related to the number average molecular weight, $\bar{M}_n$, by

$$C = \frac{2 \times 10^6}{\bar{M}_n} \qquad (10)$$

For the *IV* measured in 60/40 phenol/tetrachloroethane solvent at 25°C, C is related to $\bar{M}_n$ by the Moore[13] equation:

$$IV = 7.50 \times 10^{-4} \bar{M}_n^{0.68} \qquad (11)$$

Substituting for $\bar{M}_n$ in this equation using the relationships of eqs. (6) and (10) leads to

$$IV = 14.4465 \left[\frac{1 + 2k_a (C_0 - C_{ai})t}{C_0 + 2k_a (C_0 - C_{ai})C_{ai}t} \right]^{0.68} \qquad (12)$$

Once the values of k_a and C_{ai} are determined, the *IV* at any time during the SSP can be calculated using this equation.

Comparison with Existing Empirical Rate Equations for SSP of PET

There are several existing empirical rate equations for the SSP of PET and Nylons. To be considered as an empirical rate equation, the equation must be reasonably simple, has an analytical solution, and fits SSP data reasonably well at least within some SSP time frame or under some special SSP conditions. The adequacies of the proposed semiempirical rate equation and the following three empirical rate equations will be compared.

1. Constant rate equation—Layman's equation: this equation assumes that the IV build-up rate during SSP is constant, i.e.,

$$\frac{d(IV)}{dt} = k \qquad (13)$$

Therefore, IV is a linear function of the reaction time,

$$IV = IV_0 + kt \qquad (14)$$

where IV_0 is the prepolymer or initial IV. Equation (13) may seem like a layman's equation, but as a matter of fact, it is widely and routinely used or implied by SSP professionals because of its simplicity. For example, if it takes a PET feed polymer 10 h to solid-state polymerize from an initial IV of 0.60 dL/g to the product IV of 0.82 dL/g, then the SSP rate is given as 0.022 dL/g per hour. Because in most cases the SSP rate is faster in the early stage and slower in the later stage of the SSP, the SSP rate given is really the average rate. In some cases, the constant rate equation is actually quite reasonable. For example, in fixed-bed SSP at lower temperatures ($\leq$190°C), the IV vs. time plots are close to straight lines especially if the pellet sizes are large. In the SSP of PET in a tumble dryer under a vacuum, the IV build-up curve is almost linear until a high IV is reached. Because earlier commercial SSP of PET (for tire-cord application) was conducted in tumble dryers, the constant rate equation may have its historical origin.

2. Power-of-the-time rate equation—Walas[14] equation: Walas[14] pointed out that the rate of a process in a solid material, which involves chemical reaction and diffusion, usually varies as some power of the time, t, i.e.,

$$\text{Rate} = kt^n$$

Because SSP is such a process, the following Walas rate equation has been widely used to study the SSP of Nylons and PET, and has become the standard empirical rate equation for SSP:

$$\frac{d\bar{M}_n}{dt} = kt^n \qquad (15)$$

The solution for $\bar{M}_n$ is

$$\bar{M}_n = \bar{M}_{n0} + \frac{1}{n+1}kt^{n+1} \qquad (16)$$

The value of n is usually quite close to -0.5. Griskey and Lee[15] investigated the SSP of Nylon 66 and found the kinetic equation

$$\frac{d\bar{M}_n}{dt} = kt^{-0.49} \qquad (17)$$

approximately described the rate of molecular weight change. Chen et al.[5] equated kt^n to a rate function defined for their diffusion equation to calculate the specific reaction rates for the SSP of PET, Nylon 66, and Nylon 610. Gaymans et al.[2] used a modified form of Walas equation to fit their SSP data for Nylon 6. Dröscher and Wegner[16] conducted SSP of powdered PET with one of the two 2-hydroxyethyl ends groups in each chain substituted with a chlorine atom under a vacuum and found that the intrinsic-viscosity average molecular weight increases linearly with the square root of time. Jabarin and Lofgren[17] performed SSP experiments in a fixed bed using commercial PET prepolymers from Goodyear, Firestone, and Eastman, and found that the following equation fitted the SSP data:

$$\bar{M}_n = \bar{M}_{n0} + kt^{1/2} \qquad (18)$$

Most of these authors indicated that the reaction rate equation of the form of eq. (15) does not fit the SSP data at high conversions.

3. Simple second-order rate equation—Bamford[1] equation: Bamford and Wyane[1] first used the simple second-order rate equation (the same rate equation for transesterification in melt phase polycondensation) to fit their SSP data. Thus,
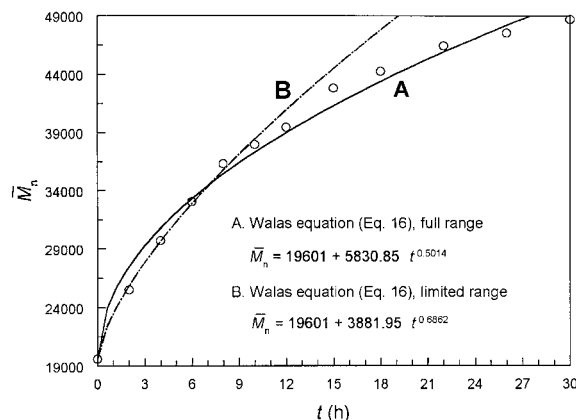
$$-\frac{dC}{dt} = 2k_a C^2 \qquad (19)$$

Figure 1   Curve fittings of Sinco SSP data with Walas equation.

Figure 3   Curve fittings of Sinco SSP data with Duh equation.

This can be considered as a special case of eq. (4) with $C_{ai} = 0$. Integrating this equation and using the initial condition yield

$$\frac{1}{C} = \frac{1}{C_0} + 2k_a t \tag{20}$$

If the Bamford rate equation fits the SSP data, then the $1/C$ versus t plot should be a straight line with slope equal to $2k_a$ and intercept equal to $1/C_0$. Bamford and Wayne[1] indicated that the apparent rate constant k_a appeared to decrease with increasing reaction time. This is another way of saying that the simple second-order rate equation does not fit the SSP data at higher conversions because k_a should remain constant during isothermal SSP. Unfortunately, an equation of this form is assumed for the forward reaction rate of transesterification in practically all the more so-
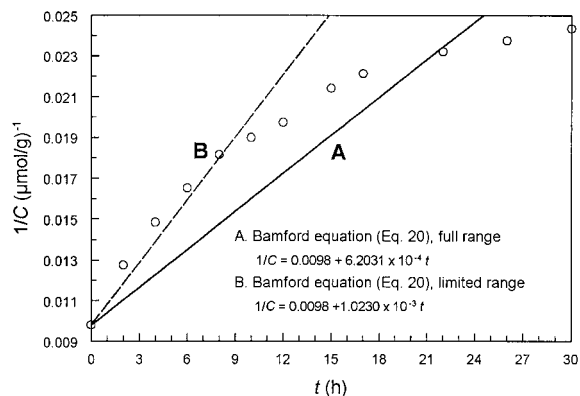
phisticated SSP models. The accuracy of this rate equation should improve if the SSP time is short, the particle size is small, or the reaction temperature is high (i.e., when C_{ai} is only a small fraction of C).

The above empirical rate equations and the proposed semiempirical rate equation (referred to as Duh equation) can be tested and compared by fitting the experimental data of a typical SSP run with each of these rate equations. Sinco Ricerche S.P.A.of Tortona, Italy, one of the three major SSP technology vendors, provided an IV vs. time plot for a typical SSP run (see Fig. 4) in their sales presentation.[18] Sinco found it "difficult to explain" the leveling-off of the IV build-up curve because they also assume rate equations of the forms of eqs. (1) and (2), which do not predict such a phe-
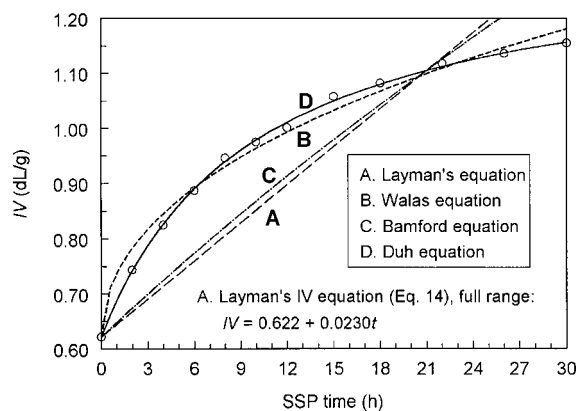

Figure 2   Curve fittings of Sinco SSP data with Bamford equation.

Figure 4   Comparison of curve fittings of full range IV data of Sinco SSP run with various empirical equations.
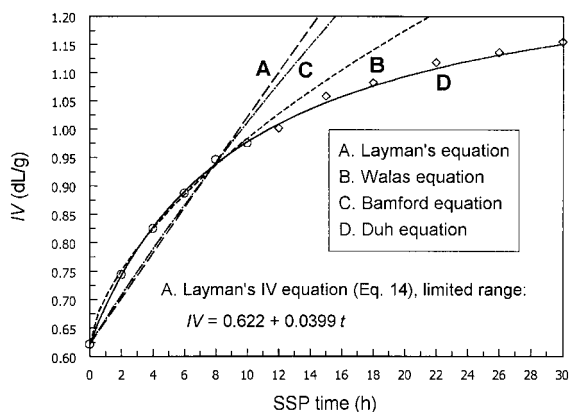
Figure 5 Comparision of curve fittings of limited range IV data of Sinco SSP run with various empirical equations.

nomenon. These SSP data will be used to compare the adequacies of the empirical rate equations discussed above.

Figure 1 shows the fittings of Walas $\bar{M}_n$ equation with the Sinco SSP data. The prepolymer used had an IV of 0.622 dL/g ($\bar{M}_{n0}$ = 19601, C_0 = 102 μmol/g). Curves A and B are obtained, respectively, when full-range data and limited-range data (for $t \leq 10$ h) are used. The fitting with full-range data is only fairly good. The fitting with limited range data is much better within the narrower time frame. Note that the power of t in eq. (16) fitted with full-range data is very close to 0.5, meaning that the value of n is very close to -0.5.

Figure 2 shows the fittings of Bamford equation [eq. (20)] with the Sinco SSP data. It can be seen that the fitting is not very good with limited-range data, and even worse with full-range data. Figure 3 shows the fittings of Duh equation with the Sinco SSP data. The fittings are excellent with both full-range and limited-range data. The fittings of Layman's equation with full-range and limited-range data are included in Figures 4 and 5, respectively.

Table I lists the values of the parameters for various empirical rate equations. The values of the parameters are used to obtain the IV build-up curves in Figures 4 and 5 for the four empirical equations. In Figure 4, the curves are based on full-range data fittings, and in Figure 5, the curves are based on limited-range data fittings.

It can be seen, in both figures, Layman's IV equation and Bamford IV equation fit the IV data poorly. This means that Layman's rate equation and Bamford rate equation are not adequate for typical SSP.

Walas IV equation fits the IV data well within limited range ($t \leq 10$ h), but not very well over the full range. Note that Walas IV equation fitted with limited-range data (referring to curve B in Fig. 5) deviates widely from the data outside the limited range (for $t > 10$ h).

Duh IV equations fit the IV data well in both Figures 4 and 5. It is worth noting that, in Figure 5, although the IV vs. time curve for Duh equation is based on limited-range data fitting, it fits all the data well. This indicates that Duh equation can be extrapolated to predict the IV values well beyond the actual experimental time with reasonable accuracy. In this particular example, the SSP experiment could have been terminated after 10 h, and Duh equation fitted with the IV data of the samples taken within the 10-h experimental time would still satisfactorily predict the product IV after up to 30 h of SSP. Because all the other empirical equations, including Walas equation, predict ever-increasing IV, extrapolations of these equations are usually unreliable. It is understood that reasonably accurate experimental data are required for a good fit—no empirical equation can satisfactorily fit experimental data that scatter widely.

Table I   Values of Parameters for Various Empirical Rate Equations Fitted with Sinco SSP Data

Empirical Equations	Full-Range Data Fitting		Limited-Range Data Fitting	
	k or k_a	C_{ai} or n	k or k_a	C_{ai} or n
Layman's	[eq. (13)] k = 0.0230 (dL/g)(h)$^{-1}$		k = 0.0399 (dL/g)(h)$^{-1}$	
Walas	[eq. (15)] k = 2923.59 (h)$^{-0.5014}$	$n = -0.4986$	k = 2663.79 (h)$^{-0.6862}$	$n = -0.3138$
Duh	[eq. (4)] k_a = 1.8620 × 10^{-3} (μmol/g)$^{-1}$ (h)$^{-1}$	C_{ai} = 33.51 (μ mol/g)	k_a = 1.9022 × 10^{-3} (μ mol/g)$^{-1}$ (h)$^{-1}$	C_{ai} = 33.05 (μ mol/g)
Bamford	[eq. (19)] k_a = 3.1016 × 10^{-4} (μ mol/g)$^{-1}$ (h)$^{-1}$		k_a = 5.1150 × 10^{-4} (μ mol/g)$^{-1}$ (h)$^{-1}$	

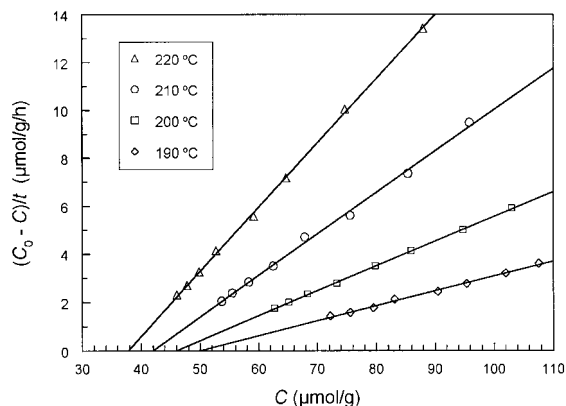**Figure 6** $(C_0 - C)/t$ vs. C plots for SSP of PET at various temperatures.

Figure 7 IV build-up curves for SSP of PET at various temperatures.

EXPERIMENTAL

Four SSP runs were conducted at different temperatures (190, 200, 210, and 220°C) to generate data to test the proposed SSP rate equation (referred to as Duh equation) for the temperature effect. The prepolymer used was DMT-based PET with an IV of 0.574 dL/g, a pellet size of 0.02 g, a carboxyl end group concentration of 18 μmol/g, and a methyl end group concentration of 3 μmol/g. Note that the methyl end groups behave as inactive end groups during SSP. The reactor used to conduct the SSP runs was constructed of a 50-cm long glass column with a diameter of 37 mm. The reactor had a cone-shaped bottom, which was connected to a 7-mm diameter, 150-cm long nitrogen supply tube, which was coiled up around the lower half of the reactor column. During the experimental runs, the reactor with its nitrogen supply tube was immersed in a constant temperature oil bath about 30-cm deep. The nitrogen supply tube also served as a heat exchanger, which heated the incoming nitrogen to the desired experimental temperatures.

About 100 g of prepolymer was used for each run. The prepolymer was first crystallized and dried at 160°C for 2 h with a nitrogen stream passing through the reactor at a flow rate of 7 standard liters per minute (SLPM). Then the polymer temperature was raised to the desired reaction temperature to effect SSP, which lasted for 30 h. Samples were taken at various intervals to monitor the IV change during the SSP. The IV data for the four SSP runs at various temperatures can be found in Figure 7.
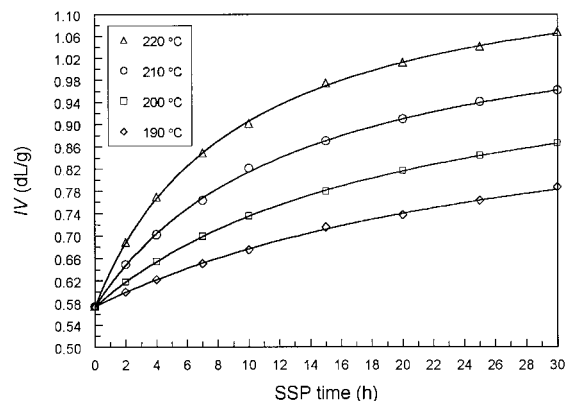
RESULTS AND DISCUSSION

To test the proposed rate equation for the effect of SSP temperature, the IV data obtained from the above SSP experiments are used. To test the proposed rate equation for the effects of other factors, published SSP data are used.

Effect of Temperature on SSP Rate

The IV data obtained from the above SSP experiments are used to prepare the $(C_0 - C)/t$ vs. C plots in Figure 6 for the four SSP runs at different temperatures. At $IV_0 = 0.574$ dL/g, $C_0 = 114.83$ μmol/g. Four straight lines are obtained, indicating that the proposed rate equation fits the SSP data well for all the four SSP runs. The four straight lines are represented by the following equations for various SSP temperatures:

$$(C_0 - C)/t = 0.0616C - 3.0787 \quad \text{for 190°C}$$

$$(C_0 - C)/t = 0.1032C - 4.7441 \quad \text{for 200°C}$$

$$(C_0 - C)/t = 0.1731C - 7.2672 \quad \text{for 210°C}$$

$$(C_0 - C)/t = 0.2678C - 10.1003 \quad \text{for 220°C}$$

Table II   Values of k_a and C_{ai} for Various SSP Temperatures

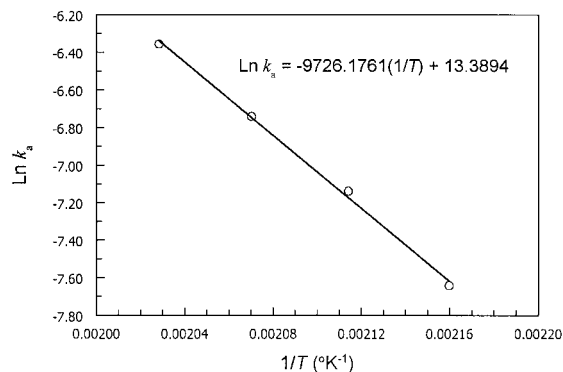| SSP temp. (°C)	k_a $(\mu$mol/g$)^{-1}$ (h)$^{-1}$	C_{ai} (μmol/g)
190	4.7497×10^{-4}	49.98
200	7.4939×10^{-4}	45.97
210	1.1882×10^{-3}	41.98
220	1.7365×10^{-3}	37.72

Figure 8 Arrhenius Plot for SSP of PET.

From these equations, the values for k_a and C_{ai} are determined for each SSP temperature. Table II lists the values of k_a and C_{ai} for the four SSP temperatures.

As expected, the apparent rate constant k_a increases with increasing temperature. This is readily understood because the SSP rate should increase with increasing temperature. As the temperature is increased, the mobility and activity of the chain ends are also increased, resulting in an increased overall forward reaction rate constant. The apparent inactive end group concentration C_{ai} decreases with increasing temperature because of two reasons. First, as the temperature is increased, some of the inactive end groups are sufficiently activated and become active. In other words, some of the end groups trapped in the crystalline phase are rejected into the amorphous phase as a result of the increasing "fractionating" action of polymer crystallization at a higher temperature. Second, as the temperature is increased, the diffusion resistance, which is accounted for mainly by the apparent inactive end group concentration according to the proposed model, decreases. As a result of increased byproduct diffusivities, byproduct concentrations within the pellets decrease. This, in turn, decreases the backward reaction rates and increases the net SSP rate. The increased diffusion rates and decreased backward reaction rates are accounted for by the increased k_a and decreased C_{ai}.

The values of k_a and C_{ai} can be substituted in eq. (12) to express IV as a function of SSP time for each SSP temperature. The IV equations thus obtained are plotted in Figure 7 for the four SSP temperatures. It can be seen that the curve fittings are very good for all of the four SSP temperatures. Note that the IV build-up curve for 190°C

is close to a straight line, especially within a limited time frame.

Figure 8 shows the Arrhenius plot for the apparent rate constant using the k_a values in Table II. A straight line is obtained. Therefore, the temperature dependence of the apparent rate constant can be represented by the Arrhenius equation,

$$k_a = A \, \exp\left\{\frac{-E_a}{RT}\right\} \qquad (21)$$

where A is the frequency factor, E_a, the apparent activation energy, T the absolute temperature, and R, the universal gas constant. From the intercept and the slope of the straight line in Figure 8, the values of A and E_a are determined to be

$$A = 653,044(\mu mol/g)^{-1}(h)^{-1};$$

$$E_a = 19,326 \text{ cal/mol}$$

In Figure 9, apparent inactive end group concentration C_{ai} is plotted against absolute temperature, T. A straight line represented by the following equation is obtained:

$$C_{ai} = 238.79 - 0.4077 \, T \qquad (22)$$

This equation shows that C_{ai} decreases linearly with the SSP temperature.

With k_a and C_{ai} available as functions of SSP temperature, the IV can be expressed as a function of SSP time and temperature. A general IV equation thus obtained may be used to estimate the IV of the product solid stated for any period of time within 30 h at any temperature between 190 and 220°C.
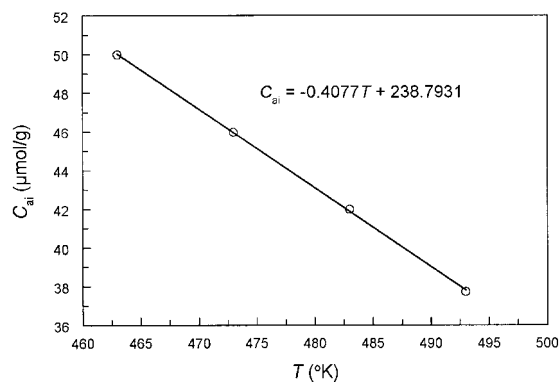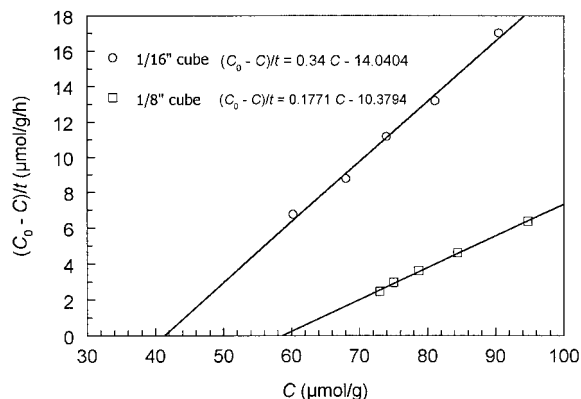

Figure 9 C_{ai} vs. T plot for SSP of PET.

Figure 10 $(C_0 - C)/t$ vs. C plots for SSP of PET with different particle sizes.

Figure 11 Curve fittings of IV data for SSP of PET with two different particle sizes.

Because the SSP temperature affects both k_a and C_{ai}, the apparent activation energy, E_a, alone is not sufficient for use to compare rates at different temperatures. There are two ways to compare SSP rates at different temperatures. Most people are more interested in the average rates over a certain IV range. For example, the reaction time requirements to achieve a product IV of 0.78 dL/g are 4.4, 7.8, 15.0, and 29.1 h at 220, 210, 200, and 190°C, respectively (referring to Fig. 7). Within the temperature ranges of 190–210 and 210–220°C, the average SSP rate increases by about 93 and 77%, respectively, with each 10°C increase in temperature. Of course, the SSP rate at a certain IV (or C) can also be compared using eq. (4). For example, at an IV of 0.70 dL/g ($C = 85.76$ μmol/g), the SSP rates are 1.22, 2.37, 4.55, and 8.02 μmol/g/h, respectively, at 190, 200, 210, and 220°C. In general, the temperature effects on the rate and the average rate are quite similar.

Effect of Particle Size

The SSP data for 1/8-inch and 1/16-inch PET cubes at 220°C provided by Chang[6] will be used to test the proposed rate equation for the particle-size effect. Six data points are taken from each of the $\bar{M}_n$ build-up curves for the two particle sizes

Table III   Effects of Particle Size on k_a and C_{ai}

Particle Size	k_a $(\mu$mol/g$)^{-1}$ (h)$^{-1}$	C_{ai} $(\mu$mol/g)
1/8-in. cube	1.8102×10^{-3}	58.61
1/16-in. cube	2.5668×10^{-3}	41.29

at 220°C. The $\bar{M}_n$ values are converted to the IV values and shown in Figure 11. The prepolymer had an initial IV of 0.60 dL/g ($C_0 = 107.53$ μmol/g). Figure 10 shows the $(C_0 - C)/t$ vs. C plots for the two particle sizes. From the equations of the two straight lines obtained, the values for k_a and C_{ai} are determined and listed in Table III.

The values of k_a and C_{ai} in Table III can be used to obtained the equations for the IV as functions of SSP time for the SSP of 1/8-inch and 1/16-inch PET cubes at 220°C, which are plotted in Figure 11. Again, the curve fittings are good.

It is obvious that the SSP rate decreases with increasing particle size. An increase in the particle size increases not only the diffusion resistance to the reaction byproducts, EG and water, but also the byproduct concentrations within the polymer particles, which in turn, increase the backward reaction rates of transesterification and esterification. These effects are reflected by the increased C_{ai} and the decreased k_a.

Effect of Prepolymer IV

Bamford and Wayne[1] reported that, in SSP, there is a limit to the increase in IV, which can be obtained with any given initial polymer. If after the SSP, a specimen that has reached its limiting IV is remelted, quenched, and then broken up, further polymerization becomes possible. They further indicated that the apparent rate constant increases with increasing prepolymer IV, but did not offer an explanation. Moore et al.[19] received a U.S. patent based on similar principles. The invention was illustrated by the following example. A powdered PET prepolymer with an IV of about 0.27 dL/g and a particle size in the range of 300–
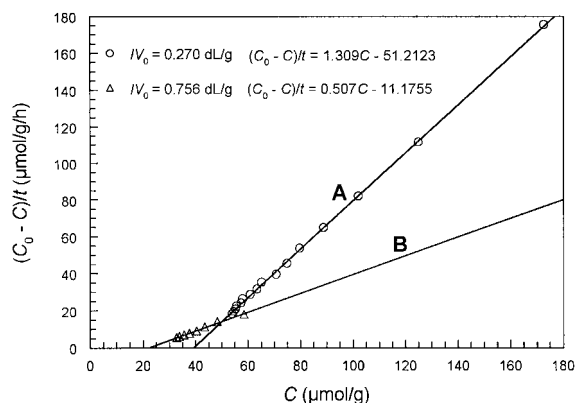
Figure 12 $(C_0 - C)/t$ vs. C plots for SSP of two pre-polymers with different IV values.

Figure 13 IV Build-up curves for SSP of two prepolymers with different IV values.

600 μm was solid-state polymerized in a fixed-bed reactor at 215°C for 16 h (referring to curve A in Fig. 13). After an initial rapid increase in IV, the rate decreased drastically. After 8 h of the SSP, a portion of the PET powder was removed, melted, quenched, ground, crystallized at 130°C for 30 min, and solid-state polymerized under identical conditions as the original polymer powder (referring to curve B in Fig. 13). It is readily apparent that the remelted and recrystallized polymer regained a high polycondensation activity and attained a much higher IV, after a total of 16 h of SSP, than possible with the original polymer.

According to Duh,[12] to achieve reaction-controlled SSP, the particle size must be reduced to below 250 μm. Therefore, there was still substantial diffusion resistance within the polymer particles. When a solid-stated polymer is remelted, the existing morphology is destroyed and the molecular weight distribution is randomized, resulting in a polydispersity of a melt polymer. Therefore, the remelted polymer in the example became a new prepolymer with a higher IV (0.756 dL/g).

Figure 12 shows the $(C_0 - C)/t$ vs. C plots for the two prepolymers with different IV values. Two straight lines are obtained. From the slope and the C intercept of each straight line, values of k_a and C_{ai} are determined (see Table IV). It is

Table IV   Effects of Prepolymer IV on k_a and C_{ai}

Prepolymer IV (dL/g)	k_a $(\mu mol/g)^{-1}(h)^{-1}$	C_{ai} $(\mu mol/g)$
0.27	2.1181×10^{-3}	39.12
0.756	4.6805×10^{-3}	22.04

obvious that k_a increases and C_{ai} decreases with increasing prepolymer IV. Similar observations have been explained by Duh[12] in terms of crystalline structure and chain mobility. As mentioned earlier, most inactive end groups are trapped in the crystalline structure. Because a lower IV prepolymer has a higher end-group concentration, statistically, a greater number of end groups will be trapped and rendered inactive in a unit mass of a lower IV prepolymer. Because it is easier for shorter polymer chains to fit into the crystal lattices, a lower IV prepolymer tends to form more regular and rigid crystals and achieve a higher degree of crystallinity. Therefore, the molecular chains of a higher IV prepolymer on average have a higher mobility. As a result, a higher IV prepolymer will have a greater k_a.

Because the higher IV prepolymer (Prepolymer B) has a greater k_a and a smaller C_{ai} than the lower IV prepolymer (Prepolymer A), it will have a higher SSP rate at any fixed IV. For example, at $IV = 0.756$ dL/g (the initial IV of Prepolymer B), the SSP rates of Prepolymers A and B are 5.94 and 27.85 μmol/g/h, respectively. This means that by remelting the solid stated product of Prepolymer A after 8 h of SSP and performing the SSP again, the SSP rate can be increased by almost 400%. Furthermore, based on the C_{ai} values, Prepolymer B can attain an ultimate IV of 1.76 dL/g, while Prepolymer A can only attain an ultimate IV of 1.19 dL/g.

The values of k_a and C_{ai} in Table IV are used to obtain the IV equations for the two prepolymers, which are plotted in Figure 13. It can be seen that the curve fittings are very good. It is appropriate to point out here a common mistake, which is sometimes made in estimating the SSP time re-
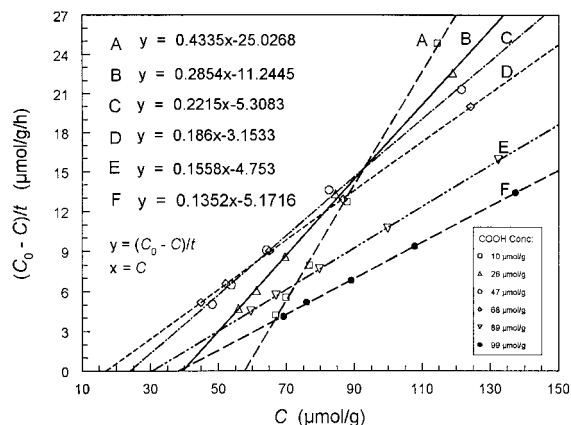
Figure 14 $(C_0 - C)/t$ vs. C plots for SSP of prepolymers with various carboxyl concentrations.

Figure 15 Effect of prepolymer carboxyl concentration on apparent rate constant for SSP of PET.

quired for a lower *IV* prepolymer to achieve a certain product *IV* based on that for a higher *IV* prepolymer. For example, because it takes Prepolymer B about 1.3 h to polymerize from 0.756 to 0.95 dL/g and it takes Prepolymer A about 5.5 h to polymerize from 0.27 to 0.756 dL/g (referring to Fig. 13), most people would estimate that it takes prepolymer A about 6.8 h to polymerize from 0.27 to 0.95 dL/g. In fact, it takes about 15 h.

Effects of Prepolymer Carboxyl Concentration

The concentration of the carboxyl end groups in the prepolymer has a great effect on the SSP rate of PET. This has been discussed in two U.S. patents to Duh.[20,21] The first Duh patent[20] demonstrates that in the SSP of powdered PET, wherein diffusion resistance is small or negligible, the highest SSP rate is achieved with zero carboxyl concentration, and the SSP rate decreases monotonously with increasing prepolymer carboxyl concentration. This indicates that the presence of carboxyl end groups reduces the combined rate of
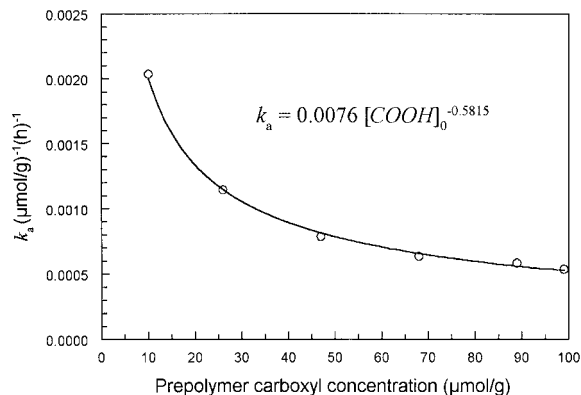
polycondensation reactions (transesterification and esterification). The second Duh patent[21] demonstrates that, in the presence of substantial diffusion resistance (as in the SSP of pelletized PET), there exists an optimal prepolymer carboxyl concentration for the fastest overall SSP rate. This is because the presence of diffusion resistance favors esterification, which generates a byproduct (water) with a higher diffusivity than the byproduct of transesterification (EG).

The *IV* data points shown in Figure 17 for the SSP of PET prepolymers with carboxyl concentrations ranging from 10 to 89 μmol/g at 230°C are taken from the second Duh patent.[21] The *IV* data for the prepolymer with a carboxyl concentration of 99 μmol/g, which do not appear in this patent, are included for this study to expand the carboxyl concentration range. All the prepolymers contained 5 ppm Ti catalyst and had *IV* values of about 0.45 dL/g and pellet sizes of about 0.01 g. Figure 14 shows the $(C_0 - C)/t$ vs. C plots for the six prepolymers with different carboxyl concentrations. From the equations of the six straight lines obtained, the values of C_{ai} and k_a are determined and listed in Table V.

Table V   Values of k_a and C_{ai} for SSP of Prepolymers with Various Carboxyl Concentrations

Prepolymer Carboxyl Conc. (μmol/g)	Prepolymer [COOH]/[OH] Ratio	k_a $(\mu$mol/g$)^{-1}$ (h)$^{-1}$	C_{ai} (μmol/g)
10	0.06	2.0350×10^{-3}	57.73
26	0.19	1.1430×10^{-3}	39.40
47	0.40	7.8952×10^{-4}	23.97
68	0.71	6.3142×10^{-4}	16.95
89	1.19	5.8252×10^{-4}	30.51
99	1.52	5.3650×10^{-4}	38.25

The values of k_a and C_{ai} in Table V are plotted against the prepolymer carboxyl concentration in Figures 15 and 16, respectively. It can be seen in Figure 15 that the value of k_a decreases monotonously with increasing prepolymer carboxyl concentration and can be fitted with a power function of prepolymer carboxyl concentration, $[COOH]_0$. The decrease in k_a reflects the decrease in the combined rate of chemical reactions due to the increase in carboxyl concentration as explained in the first Duh patent.[20] In Figure 16, it is obvious that C_{ai} decreases as the prepolymer carboxyl concentration is increased from a low value, reaches a minimum at a prepolymer carboxyl concentration of about 65 μmol/g , and then increases as the prepolymer carboxyl concentration is further increased. It can be seen that C_{ai} can be fitted reasonably well with a second-order polynomial function of prepolymer carboxyl concentration. The decrease in C_{ai} with increasing prepolymer carboxyl concentration up to about 65 μmol/g reflects the decrease in the overall byproduct diffusion resistance as a result of the increasing contribution of esterification to the overall polycondensation. As the prepolymer carboxyl concentration is further increased, there are insufficient hydroxyl ends to react with all the carboxyl ends, and more of the carboxyl ends will behave as dead ends. This effect is accounted for by the increase in C_{ai}.

The values of C_{ai} and k_a in Table V are used to obtain the IV equations for the six prepolymers with different carboxyl concentrations, which are plotted in Figure 17. It can be seen that in the early stage of the SSP, the SSP rate increases with decreasing prepolymer carboxyl concentra-
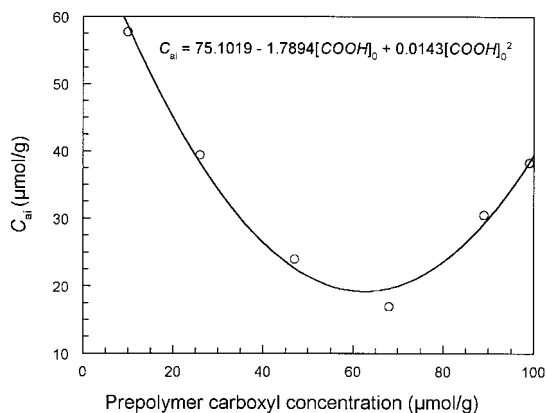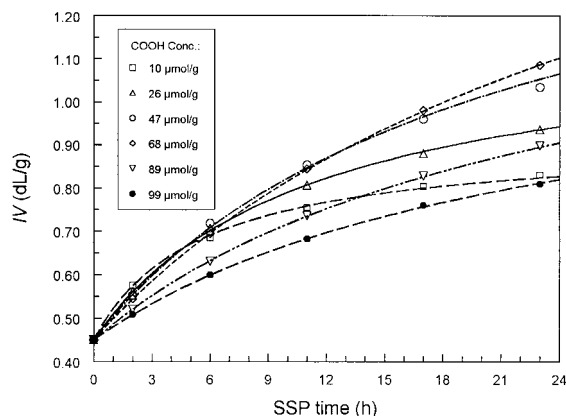

Figure 17 *IV* build-up curves for SSP of prepolymers with various carboxyl concentrations.

tion. This is because initially most of the polycondensation takes place near the pellet surfaces where diffusion resistance is small and end group reaction rate is more important than byproduct diffusion rate. As the SSP is continued, more and more polycondensation takes place deeper inside the pellets, where the byproduct diffusion resistance becomes substantial. As a result, the SSP rates of lower carboxyl prepolymers are overtaken by those of some higher carboxyl prepolymers (because the SSP rates of lower carboxyl prepolymers decrease more rapidly than those of higher carboxyl prepolymers). Therefore, the optimal prepolymer carboxyl concentration for the fastest average SSP rate (or the shortest residence time requirement) depends on the product IV (or ΔIV). For example, the optimal prepolymer carboxyl concentrations for product IV values of 0.62, 0.72, and 0.82 dL/g are 0, 45, and 53 μmol/g respectively.

CONCLUSIONS

A semiempirical rate equation has been satisfactorily tested for the SSP of PET under various conditions. This rate equation is based on a model, which assumes that there are two categories of end groups in PET during SSP, active and inactive end groups, and the overall SSP follows a second order kinetics. Thus, the proposed rate equation contains two parameters, apparent reaction rate constant, k_a, and apparent inactive end group concentration, C_{ai}. With this model, it is not necessary to explicitly distinguish the two kinds of functional end groups, hydroxyl and carboxyl end groups, and the two types of polycon-

Figure 16 Effect of prepolymer carboxyl concentration on apparent inactive end group concentration for SSP of PET.

densation reactions, transesterification and esterification, with their respective byproducts, EG and water. Nor is it necessary to explicitly break down the SSP process into the reaction step and the diffusion step. Instead, the effects of all the factors that influence the SSP rate are implicitly and conveniently accounted for by the two parameters. For example, k_a increases while C_{ai} decreases with increasing SSP temperature, increasing prepolymer IV, and decreasing particle size. The effects of the prepolymer carboxyl concentration are a bit more complex. Although k_a always decreases with increasing prepolymer carboxyl concentration, C_{ai} decreases as the prepolymer carboxyl concentration is increased from a low value to an intermediate value and then increases as the prepolymer carboxyl concentration is further increased.

The proposed rate equation appropriately describes the behaviors of the SSP of PET and fits the IV or molecular weight build-up curves for SSP under various conditions very well. Furthermore, it can be extrapolated with reasonable accuracy. The success of this rate equation can be attributed to three reasons. First, it is basically a second-order kinetic equation with respect to the active end group concentration, similar to that for the melt-phase polymerization. Second, the form of the equation is very versatile in fitting SSP curves with a wide variety of curvatures. Third, the inclusion of the parameter C_{ai} aptly predicts the existence of the ultimate IV or molecular weight achievable by the SSP.

Undoubtedly, the proposed rate equation can be satisfactorily applied to the SSP of other polyesters, such as poly(butylene terephthalate), poly(napthalene terephthalate), and poly(trimethylene terephthalate). Because of the striking similarities between solid-state polycondensation and solid-state polyamidation, it is expected that an empirical rate equation of similar form can also satisfactorily fit the SSP curves of polyamides, such as Nylon 6, Nylon 66, and Nylon 610, etc.

REFERENCES

1. Bamford, C. H.; Wayne, R. P. Polymer 1969, 10, 661.
2. Gaymans, R. J.; Amirtharaj, J.; Kamp, H. J Appl Polym Sci 1982, 27, 2513.
3. Chen, S.-A.; Chen, F.-L. J Polym Sci A: Polym Chem 1987, 25, 533.
4. Devotta, I.; Mashelkar, R. A. Chem Eng Sci 1993, 48, 1859.
5. Chen, F. C; Griskey, R. G.; Beyer, G. H. AIChE J 1969, 15, 680.
6. Chang, T. M. Polym Eng Sci 1970, 10, 364.
7. Cai, F.; Chen, M.; Tang, X. Shiyou Huagong 1990, 19, 11.
8. Ravindranath, K.; Mashelkar, R. A. J Appl Polym Sci 1990, 39, 1325.
9. Tang, Z. L.; Qiu, G.; Huang, N. X.; Claudio, S. J Appl Polym Sci 1995, 57, 473.
10. Kang, C. K. J Appl Polym Sci 1998, 68, 837.
11. Mallon, F. K.; Ray, W. H. J Appl Polym Sci 1998, 69, 1233.
12. Duh, B. J Appl Polym Sci 2001, 81, 1748.
13. Moore, L. D., Jr. ACS Meeting, Cleveland, Apr., 1960, 1, 234.
14. Walas, S. M. Reaction Kinetics for Chemical Engineers; McGraw-Hill: New York, 1959, 129.
15. Griskey, R. G.; Lee, B. I. J Appl Polym Sci 1966, 10, 105.
16. Dröscher, M.; Wegner, G. Polym 1978, 19, 43.
17. Jabarin, S. A.; Lofgren, E. A. J Appl Polym Sci 1986, 32, 5315.
18. Sales Presentation of PET SSP Technology 2000, Sinco Ricerche S.P.A., Tortona, Italy.
19. Moore, l. D.; Rule, M; Wicker, T. H. U.S. Pat. 4,446,303, May 1, 1984.
20. Duh, B. U.S. Pat. 4,205,157, May 27,1980.
21. Duh, B. U.S. Pat. 4,238,593, Dec. 9, 1980.